


Quantum chaotic features of the spin-orbit coupled excitons in disordered two-dimensional insulators

V. A. Stephanovich , E. V. Kirichenko, and K. Książek
Institute of Physics, University of Opole, Oleska 48, 45-052, Opole, Poland

Jackie Harjani Saucedo  and Belén López Brito
Department of Mathematics, Universidad de Las Palmas de Gran Canaria, Campus de Tafira Baja, Las Palmas C.P. 35017, Spain



(Received 31 January 2024; accepted 16 July 2024; published 2 August 2024)

We study the synergy between disorder (phenomenologically modeled by the introduction of Riesz fractional derivative in the corresponding Schrödinger equation) and spin-orbit coupling (SOC) on the exciton spectra in two-dimensional (2D) semiconductor structures. We demonstrate that the joint impact of “fractionality” and SOC considerably modifies the spectrum of corresponding “ordinary” (i.e., without fractional derivatives) hydrogenic problem, leading to the non-Poissonian statistics of the adjacent level distance distribution. The latter fact is strong evidence of the possible emergence of quantum chaotic features in the system. Using analytical and numerical arguments, we discuss the possibilities to control the above chaotic features using the synergy of SOC, Coulomb interaction, and “fractionality,” characterized by the Lévy index μ .

DOI: [10.1103/PhysRevE.110.024201](https://doi.org/10.1103/PhysRevE.110.024201)

I. INTRODUCTION

The advancement of ultrathin semiconducting materials technology in the last decade has spurred extensive experimental and theoretical research on amorphous and disordered structures that exhibit the physical properties required for spintronics and nanoelectronics [1–8]. The above materials can be used to fabricate low-cost photovoltaic cells, light-emitting diodes, and other electronic devices [9,10]. Even though a lot has been learned about the various aspects of exciton diffusion and dissociation in them, there are still many unanswered questions about the fundamental physics that underpin the operation of these devices, particularly concerning low-dimensional structures like surfaces and/or interfaces. For instance, it is necessary to discuss the role of the disorder in two-dimensional (2D) systems [11]. This is because the disordered semiconductors used in photovoltaics, are primarily polymers [2,6,12–14] with many kinds of conformational and other kinds of disorder. To name a few, these are different unavoidable imperfections like structural disorder, presence of chemical impurities, etc. [15], which adversely influence the functionality of a corresponding electronic device.

As the disorder is usually associated with non-Gaussian probability distributions [16–18] it is therefore natural to model it by the introduction of fractional derivatives [16,19]. In the case of quantum-mechanical problems like hydrogenic ones, the disorder can be accounted for by substitution of the ordinary Laplacian in the Schrödinger equation by the fractional one of order μ [20]. The latter equation is called the fractional Schrödinger equation [20] and at $\mu = 2$ it gives the standard one with ordinary Laplacian. Note that although weak disorder can be well treated, for strong disorder it is not the case. Under strong disorder we understand the considerable substance amorphization, leading to the disruption of

its crystalline structure so that the distances between different lattice sites become random. In such a case we also can barely speak of the energy band structure, which makes the excitonic problem in a disordered substance much less trivial [21]. In this case, the charge transfer would consist of random electron or hole hopping, very similar to the seminal Sher-Montroll model [22]. The quantization of this model leads to the path integrals over all possible quantum trajectories, however, with Lévy (rather than Gaussian, as in “ordinary” quantum mechanics) measure, containing Lévy index μ , see Ref. [20]. As we have mentioned above, Lévy index $\mu = 2$ corresponds to an ordered substance [20] while $\mu < 2$ describes the deviation from the ordered case, i.e., the degree of disorder.

Another factor, that can strongly influence the exciton properties of 2D systems, is a spin-orbit coupling (SOC). The synergy of SOC and excitons are especially notable in monolayers of transition metal dichalcogenides (TMD) like MoS_2 , WSe_2 , and WS_2 [23]. This synergy enhances the binding energy and the oscillator strength of the excitons, which permits to use SOC to manipulate their physical properties. This can be used, for instance, in photovoltaics, light-emitting diodes as well as in quantum gates [23]. At the same time, it has been shown [24,25] that adding the SOC in Rashba form [26] generates chaotic motion in the above excitons, which can degrade the performance of the above exciton-based devices. As the disorder can also adversely influence such device functionality, it is necessary to study the joint action of the above two factors on the exciton properties of the 2D structures.

In the common perception, simple quantum mechanical problems (like hydrogenic or oscillator one) have simple exact solutions. However, the possibility to solve the above problems is based exactly on the existence of underlying symmetries, reducing the number of degrees of freedom. This,

in turn, permits us to solve the problem exactly but leads to energy level degeneracies. The hydrogen problem, both in three and in two dimensions, is invariant with respect to time reversal, which is an antiunitary symmetry. When applying the above SOC and fractional derivatives, the corresponding quantum-mechanical problem loses the above antiunitary symmetry and can no longer be solved exactly. In this case, so-called quantum chaotic behavior may appear. Quantum chaos (QC) refers to the properties of quantum systems whose classical counterparts exhibit irregular, random behavior due to extreme sensitivity to their initial conditions [27]. One of the peculiarities of QC is the statistical properties of the energy levels of a quantum system. Namely, if a regular (say, “nonchaotic”) quantum system exhibits a Poissonian distribution

$$p_P = \exp(-s) \quad (1)$$

of distances s between adjacent energy levels, then the chaotic system exhibits strong repulsion between energy levels, which is reflected in the non-Poissonian distribution of the above distances [28]. The peculiar feature of all non-Poissonian distributions is the maximum at the intermediate range of $s > 0$. Here we shall use the Brody distribution [29]

$$p_B = \alpha(q+1)s^q \exp[-\alpha s^{q+1}], \quad (2)$$

which interpolates between Poisson ($q = 0$) and Wigner ($q = 1$) distribution. Here, parameter q represents the degree of chaoticity in the system. It is taken (along with parameter α) from the best fit to the corresponding energy levels histogram. It had been shown by Wigner long ago (see Ref. [28] and references therein) that the statistical properties of a large number of above adjacent levels can be described by a suitable Gaussian ensemble of Hermitian random matrices. In this case, the Wigner distribution has the name of that of Gaussian orthogonal ensemble (GOE),

$$p_{\text{GOE}}(s) = 2As \exp(-As^2). \quad (3)$$

The other popular distribution is the Gaussian unitary ensemble (GUE) one,

$$p_{\text{GUE}}(s) = \frac{4B^{3/2}}{\sqrt{\pi}} s^2 \exp(-Bs^2). \quad (4)$$

The constants A and B in Eqs. (3) and (4) are also taken from the best fit to the corresponding energy levels histogram. The distributions (2)–(4) are normalized to unity $\int_0^\infty p_i(s) ds = 1$, where index i stands for B, GOE, or GUE. Below we will show that our system demonstrates highly non-Poissonian statistics of its adjacent energy levels. Moreover, as we deal with fractional Laplacian with Lévy index μ , the above distribution (2) will be the best choice. We speculate that the parameter q of Brody distribution should be related to the Lévy index μ .

In the present paper, we study the joint influence of “fractionality” (i.e., the substitution of the ordinary Laplacian with its fractional counterpart in the Schrödinger equation) and SOC on the 2D exciton properties. We show that at sufficiently strong SOC and $\mu < 2$ (fractional case), the system demonstrates the QC features like qualitative changes in its level statistics, which are well described by the Brody distribution (2). By varying the Lévy index and SOC constant,

we can manipulate the energy level statistics. The paper is organized as follows. In Sec. II, we discuss the relationship between fractional derivatives and disorder. In Sec. III, we give the theoretical details of our approach. Here, the approximate expressions for radial wave functions of 2D “fractional” hydrogenic problem are suggested. On their base, the states of the problem with SOC will be constructed. The numerical results are discussed in Sec. IV, where our main outcome is presented. Namely, we have shown that the spin-orbit coupled “fractional” 2D exciton demonstrates clear quantum chaotic feature, that is non-Poissonian statistics of its energy levels. Conclusions will be given in Sec. V.

II. DISORDER AND NON-GAUSSIAN DISTRIBUTIONS

The central question of our consideration is the relationship between fractional derivatives and disorder. The common wisdom is that disorder is a lack of regularity. In this case, the physical quantities are not under precise control so that the properties of such disordered systems are best described in terms of distribution functions. It is firmly established, that to describe the effects, related to the disorder, sufficiently broad probability distributions (like a square of the wave function of a quantum particle) should be utilized; see, e.g., the seminal Anderson’s paper [30]. As the fractional derivatives generate the non-Gaussian (e.g., Lévy) probability distributions, this gives a rough picture of the above relationship. More precisely, in the realm of statistical and condensed-matter physics [31], they are particularly useful for modeling anomalous diffusion and other processes that exhibit nonlocality and memory effects. They describe systems where the probability of extreme events is higher than what would be predicted by Gaussian (normal) distributions. The above heavy-tailed distributions are characterized by “tails” that are not exponentially bounded, meaning they have a slower decay.

The objective now is to predict global properties shared by almost all such systems, i.e., to acquire knowledge of universal features independent of the precise realization of the disorder. If a crystal has a small number of noninteracting defects and/or impurities, signifying weak disorder, then its properties are accurately described by the Gaussian distribution function. As the latter function decays rapidly, its width is usually modest so that uncommon, “highly disordered” configurations (the so-called extreme events, see above) have (very) small statistical weights and do not contribute to the observable properties of such systems. In contrast, atoms in a highly disordered material occur in random positions rather than in crystalline periodic patterns. As a result, the actual statistical weight of the above ‘highly disordered’ configurations increases, often dramatically. This large statistical weight is indeed described by the above non-Gaussian, heavy-tailed distributions. As we discussed above, a significant breach of translation symmetry in an amorphous material results in its electronic states no longer being Bloch functions. The simplest model that describes the electronic states in the highly disordered matter was introduced by Anderson [30] and leads to the famous Anderson localization phenomenon.

Specifically, Anderson’s main theorem [30] states that transport in a system stops if the condition $W \approx V$ is fulfilled. Here, W is the width of an energy distribution and V is

the mean value of the interaction potential between disorder constituents (like impurity atoms in a semiconductor) situated at the sites of a host lattice. We emphasize here that the above energy distribution is not specified, the only requirement is that it should be sufficiently wide. Put differently, all states are strongly localized in a system with the above significant disorder. In our approach, the term “disordered lattice” refers to a high degree of disorder, which occurs in the case of large impurity concentrations, where they strongly interact with each other. Contrary to the well-studied case of weak disorder with almost noninteracting impurities [32], our case cannot be studied by traditional techniques [33]; see also Ref. [21]. For such a strongly disordered system, the distribution function of its physical characteristics is barely Gaussian, rather it has long tails, inherent in Lévy distributions.

It can be shown that the substitution $t \rightarrow it$ (i is an imaginary unit) converts the Eq. (1) of the original Anderson paper [30] to Langevin equation, which describes the random particle motion

$$\dot{\mathbf{r}} = -\lambda \nabla V(\mathbf{r}) + \mathbf{s}(t), \quad (5)$$

where λ is a dimensional factor, $\dot{\mathbf{r}} = d\mathbf{r}/dt$, ∇ is an ordinary gradient operator, acting on the potential function V , which depends on the two-dimensional (in our case) position vector $\mathbf{r} = (x, y)$. The stochastic motion is described by the random force $\mathbf{s}(t)$ with predefined statistical properties. As here we are dealing with non-Gaussian probability distributions, it is reasonable to assume, that $\mathbf{s}(t)$ obeys Lévy statistics. It is well-known [19] that for latter statistics, the probability density function (pdf) is best defined through its characteristic function (Fourier image)

$$f(k) = \exp\left(-\frac{\sigma^\mu k^\mu}{\mu}\right), \quad (6)$$

where $k \equiv |k|$ and Lévy index $0 < \mu < 2$. For $\mu = 2$ we obtain the Gaussian pdf with variance σ . In other words, the pdf (6) serves as the (one of possible) quantitative definition of the above Anderson’s distribution so that its width W can be regarded as a degree of localization in a system.

As both Eq. (1) of the paper [30] and Langevin equation (5) are stochastic differential equations, the usual approach is to extract the pdf $q(\mathbf{r}, t)$, which completely defines the corresponding stochastic dynamics. This is done using the (fractional in our case) Fokker-Planck equation

$$\dot{q}(\mathbf{r}, t) = \lambda \nabla [q(\mathbf{r}, t) \nabla V(\mathbf{r})] - Q_\mu |\Delta|^{\mu/2} q(\mathbf{r}, t), \quad (7)$$

where Q_μ is a generalized diffusion coefficient, which depends on Lévy index μ . Also, $|\Delta|^{\mu/2}$ is a two-dimensional fractional Laplacian

$$|\Delta|^{\mu/2} f(\mathbf{r}) = -A_\mu \int \frac{f(\mathbf{u}) - f(\mathbf{r})}{|\mathbf{u} - \mathbf{r}|^{\mu+2}} d^2u, \quad (8)$$

$$A_\mu = \frac{2^\mu \Gamma(\frac{\mu+2}{2})}{\pi |\Gamma(-\mu/2)|}, \quad (9)$$

where $\Gamma(x)$ is Γ function [34]. Below we shall see that in our case $1 < \mu < 2$ rather than $0 < \mu < 2$ in the above free problem. This is related to the joint action of Coulomb and spin-orbit interactions on the free (i.e., without external potential) Lévy distribution. The integral operator (8) is

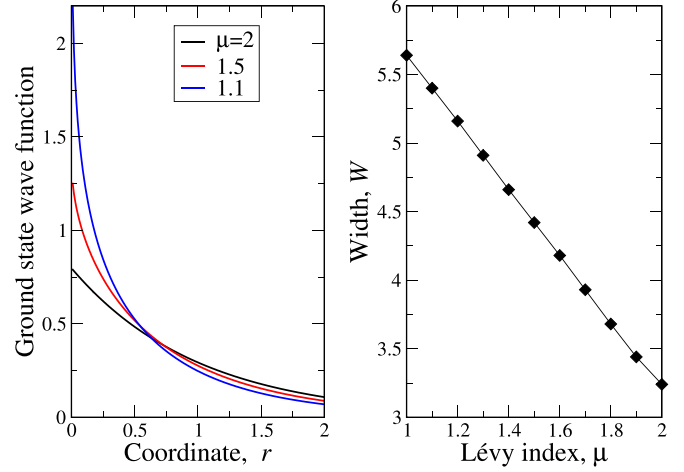


FIG. 1. The left panel shows the radial part of the ground-state wave function of the pure (without SOC) 2D fractional hydrogenic problem. The function is shown for three distinct values of Lévy index μ , coded by colors and shown in the legend. As μ decreases from $\mu = 2$ (the ordered case of the ordinary Laplacian in the Schrödinger equation) down to $\mu = 1.1$, the wave function localizes, tending to δ function at $\mu \rightarrow 1$. The right panel reports the width of the initial Lévy distribution (6).

spatially nonlocal with a slowly decaying power-law kernel (determined by the Lévy index) typical for memory effects in complex disordered systems.

The derivation of fractional Fokker-Planck equation (7) reduces to the obtaining of the pdf from the statistics of a random force; see, e.g., Ref. [35]. The same idea has also been utilized in the derivation of the fractional Schrödinger equation in Ref. [20], based on the Feynman path integral formalism [36] but with Lévy measure. Furthermore, by applying the obvious transformations $t \rightarrow it$ and $Q_{\mu=2} = \hbar^2/(2m)$ the free versions (at zero potential) of fractional Fokker-Planck and Schrödinger equations can be reduced to each other. This indicates that we can safely assume that the replacement of the underlying Gaussian distribution with a heavy-tailed one is tantamount to a phenomenological description of strong disorder in a Schrödinger equation. In this context, the Lévy index μ plays the role of a phenomenological descriptor (say, measure) of the degree of disorder. It should be noted that the above assumptions were established in Ref. [37] regarding the spectral narrowing of the nuclear magnetic resonance lineshape. The key study of Sher and Montroll [22] addresses the identical scenario.

To further demonstrate the above picture, in Fig. 1 we plot the radial part of the pure (i.e., without spin-orbit interaction) 2D hydrogenic ground-state wave function [see expression (24) below], calculated numerically by the Eq. (18) below. The left panel of Fig. 1 shows the progressive localization of the ground-state wave function as the degree of disorder (characterized by the Lévy index μ in our model) grows. The right panel reports the width of the initial Lévy distribution (6) in coordinate space. It is seen that as the width of the initial pdf (6) grows (meaning that the disorder in the system increases), the wave function becomes more and more localized, tending to Dirac delta function as $\mu \rightarrow 1$. This

shows that the conditions of Anderson theorem [30] apply to our system. This, in turn, supports our assumption that the substitution of the ordinary Laplacian by the fractional one in the Schrödinger equation effectively describes disorder.

III. THEORETICAL APPROACH

A. General formalism

We represent the Hamiltonian for our 2D “fractional” excitons with spin-orbit coupling in the form $\mathcal{H} = \mathcal{H}_0 + \mathcal{H}_{\text{so}}$. Here \mathcal{H}_0 is the Hamiltonian of 2D “fractional” spinless hydrogenic problem

$$\mathcal{H}_0 = -D_\mu |\Delta|^{\mu/2} - \frac{\beta}{r}, \quad (10)$$

where D_μ is a mass term [20] (see also below) and $\beta = e^2/\kappa$ (e is the electronic charge and κ is the dielectric constant of a host crystal). Also, here $|\Delta|^{\mu/2}$ is a two-dimensional fractional Laplacian (8).

The second term represents SOC in the Rashba form [26]

$$\mathcal{H}_{\text{so}} = \alpha_0 (p_x \sigma_y - p_y \sigma_x), \quad (11)$$

where α_0 is dimensional spin-orbit coupling constant and σ_i ($i = x, y, z$) are corresponding Pauli matrices. Here p_i ($i = x, y$) are the components of momentum operator $\mathbf{p} = -i\hbar\nabla$. We note here, that while in the fractional quantum mechanics, the momentum operator has the above ordinary form [20], the kinetic energy in momentum space reads $|\mathbf{p}|^\mu$ rather than p^2 as in ordinary quantum mechanics. This feature can be checked with the help of Lévy path integral [20] and is in accord with fractional Laplacian (8) properties, which at $\mu = 2$ gives ordinary one.

We note also, that our problem realizes some kind of competition between kinetic energy (possibly fractional at $\mu < 2$) and Rashba SOC. This means that here we have two limiting cases. The first one is the large exciton where the Rashba SOC plays a major role (even at $\mu < 2$ the Rashba term dominates at low momenta) and small excitons where kinetic energy (also at $\mu < 2$) dominates. In the intermediate regime, which corresponds to our case, both contributions are equally important. This implies that the best strategy for our problem solution is to use nonperturbative approaches like variational or purely numerical ones. Below we will realize this scenario, utilizing the variational *ansätze*, whose accuracy will be checked subsequently by direct numerical solution of the corresponding integral equations.

Subsequently we shall use modified (for the fractional case $\mu < 2$) Rydberg units [20]. In these units, we measure the energy E and coordinates \mathbf{r} in the units

$$E_{0\mu} = \left(\frac{\beta}{2\hbar}\right)^{\frac{\mu}{\mu-1}} D_\mu^{-\frac{1}{\mu-1}}, \quad r_{0\mu} = \left(\frac{2\hbar^\mu D_\mu}{\beta}\right)^{\frac{1}{\mu-1}}, \quad (12)$$

respectively. The standard Rydberg units are recovered from Eq. (12) at $\mu = 2$, when $D_2 \equiv \frac{1}{2m}$ (m is a real physical mass). Note that at $\mu = 1$ both quantities $E_{0,\mu=1}$ and $r_{0,\mu=1}$ in Eq. (12) are divergent. Below we will see that this is consistent with our problem, where a discrete spectrum only exists for $\mu > 1$ [20,38]. In the units (12), the spinless Hamiltonian (10)

renders as

$$\mathcal{H}_0 = -|\Delta|^{\mu/2} - \frac{2}{r}, \quad (13)$$

while in the spin-orbital part (11) we have $\alpha_0 \rightarrow \alpha$ and $\mathbf{p} \rightarrow \mathbf{k} = -i\nabla$, where now α is a dimensionless SOC constant.

In the presence of SOC (11), the quantum number j corresponding to the total angular momentum l (actually its z component in 2D case) becomes $j = l + \sigma_z/2$, which is related to the fact that in fractional quantum mechanics the momentum operator is similar to that in ordinary one [20].

With respect to the conservation of the total angular momentum $j = l + \sigma_z/2$, in our problem, we can also separate the angular and radial variables. This means that here we can look for the wave function of the above 2D “fractional” excitons with SOC in the form of an infinite series (cf. Ref. [39]) over a complete set of discrete eigenstates of spinless “fractional” Hamiltonian \mathcal{H}_0 (13) [40],

$$\begin{aligned} \psi_l^{[m]}(r, \varphi) = e^{i l \varphi} \sum_{n=l+1} \begin{pmatrix} c_{l,n\uparrow}^{[m]} R_{nl}(r) \\ 0 \end{pmatrix} \\ + e^{i(l+1)\varphi} \sum_{n=l+2} \begin{pmatrix} 0 \\ c_{l,n\downarrow}^{[m]} R_{n,l+1}(r) \end{pmatrix}. \end{aligned} \quad (14)$$

Here the wave function is the spinor, where index $m = 1, 2, 3, \dots$ enumerates the eigenstates for a given l in ascending energy order. In other words, here index m plays a role of the principal quantum number in our “mixed” (in the sense that the state (14) is obtained by “mixing” the initial hydrogenic states R_{nl} by SOC) problem with fixed j . As we understand that the states (14) are different for different Lévy indices μ [by virtue of $R_{n,l}(r) \equiv R_{n,l,\mu}(r)$], we suppress this index for a moment without limitation of generality. Also, the radial functions $R_{n,l}(r)$ correspond to the radial part of eigenfunctions of the Hamiltonian (13). The expansion coefficients $c_{mi}^{[m]}$ ($i = \uparrow, \downarrow$) are the eigenvectors of the following block-matrix

$$\begin{pmatrix} \mathcal{H}^{\uparrow\uparrow} & \mathcal{H}^{\uparrow\downarrow} \\ \mathcal{H}^{\downarrow\uparrow} & \mathcal{H}^{\downarrow\downarrow} \end{pmatrix} \begin{pmatrix} c_{\uparrow}^{[m]} \\ c_{\downarrow}^{[m]} \end{pmatrix} = E_m \begin{pmatrix} c_{\uparrow}^{[m]} \\ c_{\downarrow}^{[m]} \end{pmatrix}, \quad (15)$$

where we suppress indices n and l for a moment. The blocks $\mathcal{H}^{\uparrow\uparrow}$ and $\mathcal{H}^{\downarrow\downarrow}$ are the eigenvalues of the spinless Hamiltonian \mathcal{H}_0 (13),

$$\mathcal{H}^{\uparrow\uparrow} = \mathcal{H}^{\downarrow\downarrow} = E_{nl} = - \int_0^\infty R_{nl}(r) \left(|\Delta|^{\mu/2} + \frac{2}{r} \right) R_{nl}(r) r dr, \quad (16)$$

and hence are diagonal in spin subspace. Here we pay attention to the fact, that in fractional case $\mu < 2$, the orbital degeneracy of a hydrogen problem is lifted by “fractionality” so that the eigenenergy E_{nl} starts to depend on the orbital index l [40–42]. This is because for $\mu < 2$, the Runge-Lenz vector [43] is no more conserved quantity. In this case, the specific Coulomb degeneracy [43] is lifted and the energy acquires the dependence on the orbital index l . At $\mu = 2$ we recover the conservation of the Runge-Lenz vector and usual eigenenergy of 2D quantum hydrogenic problem $E_n = -1/2(n - 1/2)^2$, $n = 1, 2, 3, \dots$ [44].

The blocks $\mathcal{H}^{\uparrow\downarrow}$ and $\mathcal{H}^{\downarrow\uparrow}$ are due to SOC and hence couple spin-up and spin-down states

$$\begin{aligned}\mathcal{H}_{l,n_1,n_2}^{\uparrow\downarrow} &= \alpha \int_0^\infty R_{n_1 l}(r) \left(\frac{d}{dr} + \frac{l+1}{r} \right) R_{n_2 l+1}(r) r dr, \\ \mathcal{H}_{l,n_1,n_2}^{\downarrow\uparrow} &= \alpha \int_0^\infty R_{n_1 l}(r) \left(\frac{d}{dr} - \frac{l}{r} \right) R_{n_2 l+1}(r) r dr.\end{aligned}\quad (17)$$

The practical calculations are accomplished by the truncation of the infinite series (14) [and hence the blocks in the eigenproblem (15)] on some $n = n_{\max}$. In this case, the resulting matrix (to be diagonalized) dimensions are $2(n_{\max} - j) \times 2(n_{\max} - j)$, where (for $l = 0, 1, 2, 3, \dots$) $j = l + \langle \sigma_z \rangle / 2 \equiv m + 1/2 = 1/2, 3/2, 5/2, \dots$. Our analysis shows that good accuracy is achieved at $n_{\max} > 50$, which makes the problem quite computer intensive. Note that the above procedure for $j < 0 = -1/2, -3/2, -5/2, \dots$ completes the basis. But at zero magnetic field, the time-reversal symmetry yields $E(-j) = E(j)$, where E is the eigenenergy. This fact will be taken into account in our numerical calculations.

B. Approximate expressions for the 2D fractional hydrogen eigenfunctions

To accomplish the above calculations, we need the explicit form of the radial wave functions $R_{n,l}(r)$ for an arbitrary value of the Lévy index μ . The most profitable way to accomplish this is to pass to the momentum space in the corresponding fractional Schrödinger equation $\mathcal{H}_0 \psi = E \psi$, where \mathcal{H}_0 is given by Eq. (13); see Ref. [40] for details. As in momentum space, the fractional Laplacian converts simply to k^μ ($k \equiv |\mathbf{k}|$, see above), this (after separation of the angular and radial parts of the wave function [40]), renders the above fractional Schrödinger equation also to integral one but with much more plausible kernel

$$(k^\mu + k_0^\mu) R_{n l \mu}(k) + \frac{1}{\pi} \int_0^\infty I_l(k, k') R_{n l \mu}(k') k' dk' = 0, \quad (18)$$

where we made Lévy index μ explicit. Here the eigenenergy

$$E = -k_0^\mu \quad (19)$$

and the kernel

$$I_l(k, k') = \int_0^{2\pi} \frac{e^{ilt} dt}{\sqrt{k^2 + k'^2 - 2kk' \cos t}}. \quad (20)$$

It turns out that while it is impossible to evaluate the integral (20) analytically for arbitrary l , it is possible to do so for each $l = 0, 1, 2, \dots$ [40]. For instance,

$$I_0(k, k') = -\frac{4K(q)}{k+k'}, \quad (21)$$

$$\begin{aligned}I_1(k, k') &= -\frac{2}{kk'(k+k')} [(k^2 + k'^2)K(q) - (k+k')^2 E(q)], \\ q &= \frac{4kk'}{(k+k')^2}.\end{aligned}\quad (22)$$

Here $K(m)$ and $E(m)$ are the complete elliptic integrals of the first and second kinds respectively [34].

The integral equation (18) defines the radial eigenfunctions and corresponding eigenenergies [expressed through k_0 (19)]

of our initial (i.e., without SOC) fractional hydrogenic problem for each particular l and $n \geq l$. In other words, the equation for $l = 0$ [that with kernel (21)] gives the eigenfunctions $R_{00\mu}$ (ground state), $R_{10\mu}$, $R_{20\mu}$, etc. In its turn, the equation for $l = 1$ [that with kernel (22)] determines $R_{11\mu}$, $R_{21\mu}$, $R_{31\mu}$, etc. These functions, being converted back to r space, can be used as “building blocks” for our desired states (14). The analytical expressions for the kernels $I_l(k, k')$ render the integral equation (18) to the effective 1D form, which not only permits to solve it numerically relatively easily (as compared to that in more space dimensions), but to construct variationally the approximate basis in k space [45]. It turns out, however, that despite the relative simplicity of the numerical solution of the integral equation (18) for each specific l , it is extremely difficult to use it in our resulting problem with SOC. This is because we need to construct numerically the wave functions $R_{n l \mu}(r)$ (by also numerically doing the corresponding Fourier transformation to pass to the r space), which should be further substituted into the states (14). The numerical complexity of such a problem turns out to be higher than that for the direct numerical solution of the spectral problem for $\mathcal{H}_0 + \mathcal{H}_{\text{so}}$. That is why we shall use the numerical procedure only sporadically to check the accuracy of our approximate analytical approach, based on variational method [45].

It had been shown in Ref. [45], that the approximate orthogonal basis of the integral equation (18) can be constructed as a product of the factor $(k^2 + a^2)^{-(\mu+1)/2}$ (where a is a variational parameter and μ is the Lévy index) and a polynomial with unknown coefficients. The order of polynomial corresponds to each l value and its coefficients are determined from the mutual orthogonality conditions; see Ref. [45] for details. For example, the simplest ground-state variational function has the form (here we recover the index μ)

$$R_{00\mu}(k) = \sqrt{\frac{\mu}{\pi}} \frac{a^\mu}{(k^2 + a^2)^{(\mu+1)/2}}. \quad (23)$$

The function $R_{00\mu}(k)$ (as well as those for excited states) is normalized by the condition $2\pi \int_0^\infty R_{00\mu}^2(k) k dk = 1$. The variational parameter a can be obtained by the minimization of the energy functional, derived from the integral equation (18) [45]. This parameter is a function of Lévy index μ . The variational procedure [45] gives that this function delivers a pretty good approximation to the corresponding numerical one with the error not exceeding 2%. Paradoxically, the error is smaller in coordinate space [45], where it is around 1%. Transition to the latter space employing the inverse Fourier transform yields the following analytical expression for the ground-state wave function

$$R_{00\mu}(r) = \frac{a\sqrt{2\mu}}{2^\mu \Gamma(\frac{1+\mu}{2})} (ar)^{\frac{\mu-1}{2}} K_{\frac{\mu-1}{2}}\left(\frac{ar}{2}\right), \quad (24)$$

where $K_\alpha(z)$ is a MacDonald (modified Bessel) function [34]. The function $R_{00\mu}(r)$ as well as all other functions $R_{n l \mu}(r)$ are normalized by the condition

$$\int_0^\infty R_{n l \mu}^2(r) r dr = 1. \quad (25)$$

At $\mu = 2$, we recover the exact ground-state wave function of the 2D hydrogen atom [44]

$$R_{00\mu=2}(r) = 4e^{-2r}. \quad (26)$$

In this case, the variational parameter $a = 4$. To derive Eq. (26) from Eq. (24), we use the following relation for the MacDonald function [34]:

$$K_{1/2}(z) = \sqrt{\frac{\pi}{2z}} e^{-z}. \quad (27)$$

It turns out that the variational parameter a can be well approximated by the dependence

$$a \equiv a_{n\mu} = \frac{2f(\mu)}{n - 1/2}, \quad f(\mu) = \frac{4\sqrt{2} - \mu^{3/2}}{\mu^{3/2}}. \quad (28)$$

This yields the accuracy of the states (24) around 1%. It also turns out that in r space, the polynomials for higher excited states can be well approximated by the “ordinary” (i.e., that from the “normal” 2D hydrogenic problem [44]) confluent hypergeometric function ${}_1F_1(\dots)$ [34]. This permits to construct the complete basis of the radial functions in the coordinate space in the following form:

$$R_{nl\mu}(r) = A_{nl\mu} Q_{nl\mu} r_{n\mu}^{|l| + \frac{\mu-1}{2}} K_{\frac{\mu-1}{2}}\left(\frac{r_{n\mu}}{2}\right) \times {}_1F_1(-n + |l| + 1, 2|l| + 1, r_{n\mu}), \quad (29)$$

$$r_{n\mu} = a_{n\mu} r, \quad Q_{nl\mu} = \frac{a_{n\mu}}{(2|l|)!} \left[\frac{(n + |l| - 1)!}{(2n - 1)(n - |l| - 1)!} \right]^{1/2},$$

where $-(n - 1) < l < n - 1$, $a_{n\mu}$ is defined by Eq. (28) and $A_{nl\mu}$ is normalization constant, which is calculated from the condition (25). Note that $A_{nl\mu}$ can be evaluated analytically by reducing the MacDonald function $K_{(\mu-1)/2}$ to the hypergeometric one. But the resulting integral turns out to be so cumbersome that it is much more profitable to calculate this constant numerically every time we call the function (29). At $\mu = 2$ the constant $A_{n12} = 1$ and we arrive [with respect to the relation (27)] at the known wave functions of the 2D hydrogen atom [44].

The quantitative comparison of the behavior of the wave functions (29) with numerical ones, obtained from the integral equation (18), shows the same tendency as that from our previous work, devoted to 3D fractional harmonic oscillator [46]. Namely, for the ground-state energy, the relative error does not exceed 0.9% in our case, see the inset in Fig. 2(c) of the paper [46] for comparison. Note that contrary to the case of the fractional harmonic oscillator, here we have the domain of admissible μ values $1 < \mu < 2$ so that the above maximal error occurs at $\mu \sim 1.3$, i.e., (similar to Ref. [46]) closer to the lower μ domain boundary. For higher excited states (here we checked the energies up to $n = 4$ for all possible l values) the error is even smaller, giving in worst cases 0.7%. The detailed comparison of the wave functions (cf. Fig. 2(d) of Ref. [46]) shows that the best approximation occurs near the maximum of the corresponding curve, while at the tails

it is worse, giving maximum error around 3% in our case. But this does not influence the corresponding energies and other observable characteristics (including those involved in SOC calculations, see below) of our system. This shows that the approximation (29) delivers good approximation to the numerical values.

IV. NUMERICAL RESULTS

A. Spectrum for problem with SOC: Energy levels crossing and anticrossing

In a quantum system, whose classical analog demonstrates chaotic behavior, quantum levels anticrossing (or so-called avoided crossing) is a precursor of QC onset; see, e.g., Refs. [27,47]. Latter onset shows up in the non-Poissonian distribution of distances between adjacent energy levels (2)–(4). So, the first step to obtain the above non-Poissonian statistics is to get the system spectrum and see if there are level anticrossings in it. To be specific, here we solve the spectral problem (15) for several values of spin-orbit constant α and Lévy index μ . In this case, levels anticrossing (or crossing) might appear in the energy levels as functions of parameters μ and α . A spectrum of the problem with SOC is displayed in Fig. 2.

Figure 2(a) shows the ground-state energy E_{gs} ($j = 1/2$, $m = 1$) as a function of SOC constant α at three representative values of the Lévy index μ . It is seen that E_{gs} as a function of α decays monotonically with α growth. Moreover, the lines $E_{gs}(\alpha)$ at different μ 's go parallel to each other, i.e., neither level crossing nor anticrossing occurs. This means that in its ground state the system does not demonstrate energy levels repulsion at any μ (roughly down to $\mu = 1.1$) and α (roughly up to $\alpha = 2$), achievable for our numerical calculations. The dependence of $E_{gs}(\mu)$ at three fixed α 's is reported in the inset in Fig. 2(a). It is seen that the curves for $\alpha \neq 0$ are qualitatively similar to that for a 2D fractional hydrogenic problem with $\alpha = 0$, considered by us previously [40]. Also, at $\mu = 2$ and $\alpha = 0$ we have $E_{gs} = 4$ (Rydberg units), which is exactly the same as that for ordinary 2D hydrogen atom [44].

Three other panels of Fig. 2 report the behavior of the excited states. Figure 2(b) portrays the excited state with the lowest possible $j = 1/2$ and higher $m = 2$ and 3. Two level crossing points occur at the intersections of lines, corresponding to $m = 3$ and $\mu = 1.5$ and to $m = 2$ and $\mu = 2$ and 1.8. The points lie close to each other (at small α around 0.04) and, as our analysis shows, are related to some accidental degeneracy. The same crossings occur at lower μ values. So far no avoided level crossings (anticrossings) occur in the system. The latter appears for higher (so-called Rydberg) excited states, which is demonstrated in Figs. 2(c) and 2(d). Figure 2(c) shows that there are two anticrossing points for $\mu < 2$. It can be shown, that the anticrossing points in this case occur also for $\mu = 2$ and $\alpha \sim 1$ and $m > 10$. As such large SOC constants do not correspond to the physical situation in real substances [25], we do not report them here. As j and m increase, the number of anticrossing points also grows. This situation is shown in Fig. 2(d). Our analysis shows that at $j > 5/2$ and $m > 5$, the number of anticrossing points fluctuates randomly at $0.05 < \alpha < 2$ and $1.1 < \mu < 1.9$, i.e.,

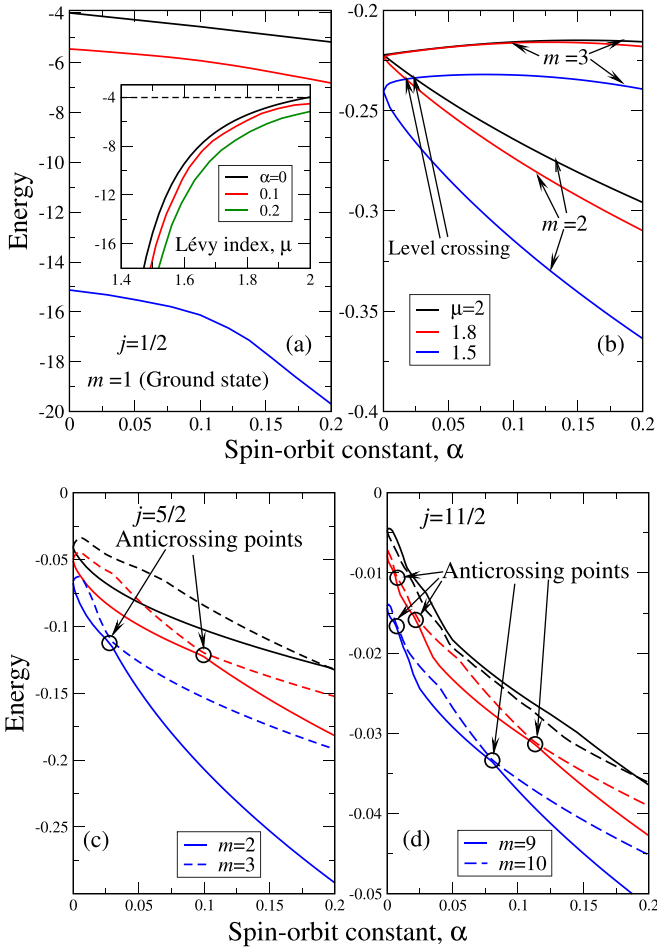


FIG. 2. (a) Shows the ground-state energy of the system for $j = 1/2$ ($l = 0$) and $m = 1$. Values of Lévy index μ are coded by colors and are shown in the legend in panel (b). This coding is the same on all four panels. Inset in panel (a) reports the dependence of ground-state energy on Lévy index μ at three fixed values of SOC constant α , shown in the legend. The black curve, corresponding to $\alpha = 0$ is exactly similar to that in “pure” (i.e., without SOC) 2D fractional hydrogen problem [40]. The dashed line shows the “ordinary” (at $\mu = 2$ and without SOC) ground-state energy of 2D hydrogen [44], which equals -4 Rydberg units. Neither level crossing nor anticrossing is present. (b) Portrays low-lying excited states $m = 2$ and 3 for the same $j = 1/2$. Level crossings are indicated by the arrows, but anticrossings are absent. Panels (c) and (d) report highly excited (so-called Rydberg) states in SOC coupled “fractional” excitons for $j = 5/2$ (c) and $j = 11/2$ (d). Multiple level anticrossings [especially for the states with $m = 9$ and 10 in panel (d)] are clearly seen. Levels with different m 's are coded by line patterns and are shown in the legends.

can be even more than in Fig. 2(d). This feature is actually responsible for non-Poissonian spectral statistics, which we consider next.

B. Non-Poissonian spectral statistics

We are now in a position to study the spectral statistics of our problem. This statistics is reported in Fig. 3 for $\mu = 2$ (left panel) and $\mu < 2$ (middle and right panels). To obtain this statistics, we took the eigenvalues up to $m = 200$ for $1/2 <$

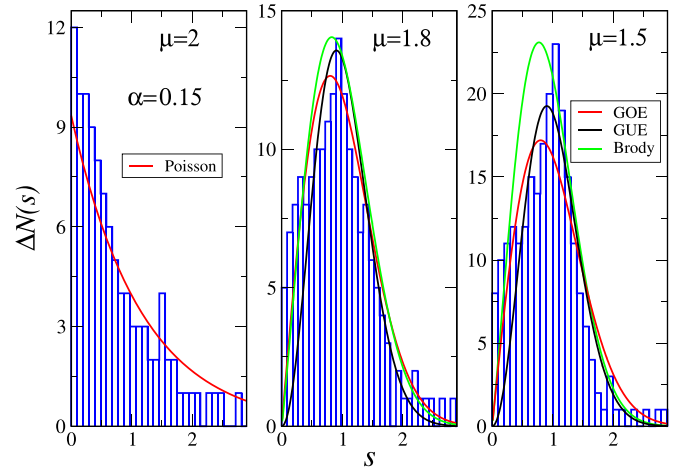


FIG. 3. Histogram for energy levels statistics for $\alpha = 0.15$ and three representative values of μ , shown in the panels. In the left panel, the red curve shows the best fit of the histogram by the (unnormalized) Poisson distribution (1). The middle and right panels report the case $\mu < 2$. In these panels, we show the best fits by the (also unnormalized) GUE (4), GOE (3), and Brody (2) distributions, coded by colors.

$j < 17/2$. This comprises around 2000 eigenvalues for each μ , which is quite a representative statistical sample. Also, to emphasize the effect of spin-orbit coupling, we took our spectral points in the interval $(-3\alpha^2, -0.55\alpha^2)$ for representative value $\alpha = 0.15$. The qualitative features of the histogram are the same for other α values at $\alpha > 0.02$, when SOC becomes pronounced. The choice of the value $-0.55\alpha^2$ for the upper bound is related to the fact that for $\mu = 2$ (nonfractional case), the continuous spectrum boundary is $-\alpha^2/2$. For $\mu < 2$ the determination of the latter boundary is a laborious problem as it requires the direct solution of the corresponding fractional differential equation. So, for our spectral statistics, we take the above “safe value” (still belonging to discrete spectra for $1.3 < \mu < 2$) for the upper bound. Also, as levels anticrossings occur primarily for the levels with the same μ , here we show the histograms for each μ separately. The qualitative shape of the “cumulative” histogram for $1.1 < \mu < 1.9$ is similar to those shown in the middle and right panels of Fig. 3.

However, the histograms for separate μ 's permit to observe an interesting feature. Namely, at μ decrease, the number and height of histogram bars for small s decrease. In other words, while at $\mu = 2$ we have the highest bars at $s = 0$, which comprises the Poissonian statistics, at $\mu < 2$ this is not the case. Rather, the highest bars shift towards the center of the histogram (around $s = 1$), signifying the strengthening of the levels repulsion. Really, as s is a difference between adjacent energy levels, $s \rightarrow 0$ means that the levels go infinitely close to each other. If we have level repulsion, then the situation when $s = 0$ becomes impossible so that $p(s = 0) = 0$, where $p(s)$ is any distribution, including the histogram. The tendency, shown in the middle and right panels of Fig. 3, shows that the larger the degree of disorder, modeled by the Lévy index μ , the more pronounced the levels repulsion or quantum chaos manifestations.

To get more insights into the properties of the histograms, in Fig. 3 we present their approximations by the GUE (4), GOE (3), and Brody (2) distributions. We use unnormalized distributions as this does not influence the qualitative conclusion about the “quantum chaoticization” of the spin-orbit coupled exciton with fractional derivatives. While for $\mu = 2$ we have only Poisson distribution (Fig. 3, left panel) with a maximum at $s = 0$, for $\mu < 2$, we have different choices. Namely, we can choose among the GOE (3) (linear asymptotics at $s \rightarrow 0$, red curves on middle and right panels of Fig. 3), GUE (4) ($\sim s^2$ at $s \rightarrow 0$, black curves), and Brody (2) ($\sim s^q$ at $s \rightarrow 0$, green curves) distributions. It is seen that the best approximations are delivered by the GUE and Brody distributions. It turns out, that for $\mu = 1.8$, the best-fit parameter of the Brody distribution $q = 1.05$, i.e., it goes very close to GOE one. The same tendency occurs at $\mu = 1.5$, where this parameter is a little more $q = 1.11$. Our analysis shows that q grows with μ decrease down to $\mu \approx 1.1$. This permits us to speculate that the parameter of Brody distribution is related to μ and thus reflects the degree of disorder in a system. We note that the Brody distribution is non-Gaussian (so-called stretched exponential) so that it may be better suited to describe the histogram, obtained in a system with underlying Lévy distribution. To emphasize the stretched exponential character of Brody distribution (2), it can be well expressed through stretched-exponential parameter $r = 1 + q$. Our independent evaluation of parameters r and q for the different regions of the energy level spacings in our problem lead for the above values of μ lead to essentially the same values. Namely, for $\mu = 1.8$ we obtained $r = 2.08$ so that $q = 1.08$, which comprises the 3% error with the previous case $q = 1.05$. At the same time, at $\mu = 1.5$, we obtain $r = 2.10$, which gives $q = 1.10$. The error in this case is smaller, giving 0.9%, but the tendency is opposite. Namely, while for $\mu = 1.8$, the parameter q turns out to be slightly higher, than its previous value, for $\mu = 1.5$ it is lower. However, the above qualitative relation between q and μ is preserved.

With regard to the above, we note the paper [48], where one more category of the energy level statistics has been considered. Namely, they examine the disordered two-dimensional topological insulator, which incorporates SOC naturally. It had been shown by Dyson long ago [49] that the energy-level statistics of the systems with broken rotational symmetry (which is the case for SOC) is described by the so-called symplectic random matrix ensemble with the strongest (as compared to above GOE and GUE) repulsion between neighboring energy levels. The strength of the repulsion may be mapped on Brody parameter $q = 4$; see, e.g., Eq. (79) of Ref. [49]. The reason that in our case Brody parameters are smaller ($q \sim 1$) may lie in the electrostatic analog of energy level repulsion, used in Ref. [49]. To be more specific, Dyson considered the 2D system with a pure 2D solution of the Poisson equation in logarithmic form. At the same time, our exciton-forming interaction is “2D sections” of ordinary 3D Coulomb interaction $\sim 1/r$ [50]. Note that both logarithmic asymptotics of the electron-hole interaction and our “2D sections” are the asymptotics of the same 2D screened (Rytova-Keldysh [51]) Coulomb interaction at large (logarithmic) and small ($1/r$) screening radii, see Ref. [52] for details. This shows, that the exact approximation of the

histograms raises many questions and controversies. We speculate here, that in our problem, the histograms can be best approximated by some kind of Lévy distribution. We postpone the detailed studies of these interesting questions for future publications.

V. DISCUSSION AND CONCLUSIONS

The main message of present consideration is that the synergy of SOC and “fractionalization” (i.e., the substitution of the ordinary Laplacian by its fractional counterpart in the Schrödinger equation) of the 2D exciton generates the quantum chaotic features in it. This becomes especially true if we recollect that the classical counterpart of the fractional Laplacian is $|\dot{\mathbf{r}}|^{\mu/(\mu-1)}$, where dot means time derivative. This generates highly nonlinear term in corresponding classical equations of motion, which alone makes the system prone to chaos. The addition of SOC only enhances these effects. Namely, our previous studies of chaos in “ordinary” (i.e., at $\mu = 2$) spin-orbit coupled 2D hydrogenic problem show that while its classical version with a kinetic energy of the form $|\dot{\mathbf{r}}|^2$ has distinct chaotic behavior with irregular system trajectories [24,53] and positive Lyapunov exponents, its quantum counterpart [25] demonstrates only weak (quantum) chaotic features. Most probably, the reason is that while (in the model with $\mu = 2$) the equations of motion are nonlinear due to the (classical version of) SOC presence, the Schrödinger equation in its quantum version is linear which may suppress the (quantum) chaotic features in the model. On the contrary, in our “fractional” case, the classical equations of motion become nonlinear due to above expression for kinetic energy. This shows that while in classical case, the “fractionality” plays secondary role (as compared to the SOC), in quantum case it plays a decisive role, generating non-Poissonian distribution of the system energy levels, as shown in Fig. 3. In other words, the introduction of fractional derivatives (i.e., Lévy underlying elementary trajectories in the sense of Feynman path integral representation [20]) highlights the quantum chaotic features in the model.

As our approximate wave functions (29) give sufficiently good accuracy to avoid much more computer-intensive direct numerical calculations, they can be readily used to calculate many observable characteristics of the excitons based on our model of spin-orbit coupled fractional Schrödinger equation. To name a few, it can be charge and spin densities, oscillator strength of the optical transitions between levels with different j (or l), spectra of light absorption, and radiative exciton lifetimes. This can be important for the above TMD monolayers [23], where disorder in the layers (“fractionality” with $\mu < 2$ in our model) can trigger the effects, which may disrupt or even destroy the functionality of corresponding electronic and spintronic devices. For instance, it can alter the exciton-exciton and exciton-phonon interactions, which can play an important role in the energy relaxation of electrons and holes, bound in an exciton. In this case, instead of a process with well-defined time dependence, the energy relaxation from a highly excited to the ground state may become chaotic. As in our model, the Lévy index μ can be used to measure the degree of disorder, we can predict (and mitigate) the detrimental influence of chaotic (and other

disorder-related features) on the physical properties of TMDs. Namely, if we fit the above experimentally observed properties in the samples with different degrees of disorder to those calculated theoretically for different μ 's, then we can extract the phenomenological dependence of μ on the degree of disorder. This, in turn, may permit to use the degree of disorder as one more control parameter to adjust the physical properties of the sample to its possible technological applications.

In this context, an interesting generalization of our problem can be suggested. Namely, we can consider possible chaos (both classical and quantum) influence on the so-called excitonic polarons, which are the exciton-phonon bound states. This problem is also important for TMD multilayer structures (where the electron can be from one layer and the hole from the other) [54], where the influence of SOC is substantial. Our preliminary analysis shows that the effects of chaos can influence drastically the optical absorption and emission spectra of the structures. To obtain the chaotic features, we should substitute the ordinary Laplacians (both in electron and phonon parts) with their fractional counterparts. Here one more question arises, namely the behavior of phonons (so-called flexural

modes [54,55]) is the disordered layer. Because of their flexural nature, such phonons would not simply localize as it was in the ordinary 2D cuts of 3D crystals (see Ref. [56]) but rather behave differently depending on their propagation direction. Moreover, our analysis shows that the nonlinearity, related to the interaction between the out- and in-plane atomic displacements (i.e., flexural phonon modes) [55] may be recast to the equivalent linear problem, but with fractional Laplacian. In other words, the flexural nature of phonons in perfectly ordered multilayer TMD structures, considered in Refs. [54,55], may be well rendered to a problem with some kind of effective disorder, which, in turn, may generate both classical (irregular electron and hole trajectories in an exciton) and quantum chaotic features. Such studies (which we defer for future publications) could help to reduce or eliminate the unwanted chaotic behavior in 2D semiconductor structures.

ACKNOWLEDGMENTS

We acknowledge support of the Julian Schwinger Foundation for Physics Research through Grant No. JSF-22-10-0001.

-
- [1] M. Bibes, J. E. Villegas, and A. Barthelémy, Ultrathin oxide films and interfaces for electronics and spintronics, *Adv. Phys.* **60**, 5 (2011).
- [2] A. Köhler and H. Bässler, *Electronic Processes in Organic Semiconductors: An Introduction*, (John Wiley & Sons, Weinheim, Germany, 2015).
- [3] A. Ohtomo and H. Y. Hwang, A high-mobility electron gas at the LaAlO₃/SrTiO₃ heterointerface, *Nature (London)* **427**, 423 (2004).
- [4] V. A. Stephanovich and V. K. Dugaev, Macroscopic description of the two-dimensional LaAlO₃/SrTiO₃ interface, *Phys. Rev. B* **93**, 045302 (2016).
- [5] M. Ansari-Rad and S. Athanasopoulos, Theoretical study of equilibrium and nonequilibrium exciton dynamics in disordered semiconductors, *Phys. Rev. B* **98**, 085204 (2018).
- [6] G. M. Akselrod, F. Prins, L. V. Poulidakos, E. M. Lee, M. C. Weidman, A. J. Mork, A. P. Willard, V. Bulović, and W. A. Tisdale, Subdiffusive exciton transport in quantum dot solids, *Nano Lett.* **14**, 3556 (2014).
- [7] M. Aßmann, J. Thewes, D. Fröhlich, and M. Bayer, Quantum chaos and breaking of all anti-unitary symmetries in Rydberg exciton, *Nat. Mater.* **15**, 741 (2016).
- [8] J. Heckötter, M. Freitag, D. Fröhlich, M. Aßmann, M. Bayer, M. A. Semina, and M. M. Glazov, Scaling laws of Rydberg excitons, *Phys. Rev. B* **96**, 125142 (2017).
- [9] M. Saliba, S. Orlandi, T. Matsui, S. Aghazada, M. Cavazzini, J.-P. Correa-Baena, P. Gao, R. Scopelliti, E. Mosconi, K.-H. Dahmen, F. De Angelis, A. Abate, A. Hagfeldt, G. Pozzi, M. Graetzel, and M. K. Nazeeruddin, A molecularly engineered hole-transporting material for efficient perovskite solar cells, *Nat. Energy* **1**, 15017 (2016).
- [10] H. Zhu, Y. Fu, F. Meng, X. Wu, Z. Gong, Q. Ding, M. V. Gustafsson, M. T. Trinh, S. Jin, and X. Y. Zhu, Lead halide perovskite nanowire lasers with low lasing thresholds and high quality factors, *Nat. Mater.* **14**, 636 (2015).
- [11] E. Abrahams, S. V. Kravchenko, and M. P. Sarachik, Metallic behavior and related phenomena in two dimensions, *Rev. Mod. Phys.* **73**, 251 (2001).
- [12] K. F. Chou and A. M. Dennis, Förster resonance energy transfer between quantum dot donors and quantum dot acceptors, *Sensors* **15**, 13288 (2015).
- [13] C. J. Bardeen, The structure and dynamics of molecular excitons, *Annu. Rev. Phys. Chem.* **65**, 127 (2014).
- [14] D. Geißler and N. Hildebrandt, Recent developments in Förster resonance energy transfer (FRET) diagnostics using quantum dots, *Anal. Bioanal. Chem.* **408**, 4475 (2016).
- [15] M. Pope and C. E. Swenberg, *Electronic Processes in Organic Crystals and Polymers* (Oxford University Press, New York, NY, 1999).
- [16] R. Metzler, J.-H. Jeon, A. G. Cherstvy and E. Barkai, Anomalous diffusion models and their properties: Non-stationarity, non-ergodicity, and ageing at the centenary of single particle tracking, *Phys. Chem. Chem. Phys.* **16**, 24128 (2014).
- [17] E. Lucioni, B. Deissler, L. Tanzi, G. Roati, M. Zaccanti, M. Modugno, M. Larcher, F. Dalfovo, M. Inguscio and G. Modugno, Observation of subdiffusion in a disordered interacting system, *Phys. Rev. Lett.* **106**, 230403 (2011).
- [18] S. A. Gredeskul and Y. S. Kivshar, Propagation and scattering of nonlinear waves in disordered systems, *Phys. Rep.* **216**, 1 (1992).
- [19] R. Metzler and J. Klafter, The restaurant at the end of the random walk: Recent developments in the description of anomalous transport by fractional dynamics, *J. Phys. A: Math. Gen.* **37**, R161 (2004).
- [20] N. Laskin, *Fractional Quantum Mechanics* (World Scientific, Singapore, 2018).
- [21] B. I. Shklovskii and A. L. Efros, *Electronic Properties of Doped Semiconductors* (Springer, Berlin, 1984).
- [22] H. Scher and E. W. Montroll, Anomalous transit-time dispersion in amorphous solids, *Phys. Rev. B* **12**, 2455 (1975).

- [23] G. Wang, A. Chernikov, M. M. Glazov, T. F. Heinz, X. Marie, T. Amand and B. Urbaszek, Excitons in atomically thin transition metal dichalcogenides, *Rev. Mod. Phys.* **90**, 021001 (2018).
- [24] V. A. Stephanovich and E. Y. Sherman, Chaotization of internal motion of excitons in ultrathin layers by spin-orbit coupling, *Phys. Chem. Chem. Phys.* **20**, 7836 (2018).
- [25] V. A. Stephanovich, E. Y. Sherman, N. T. Zinner and O. V. Marchukov, Energy-level repulsion by spin-orbit coupling in two-dimensional Rydberg excitons, *Phys. Rev. B* **97**, 205407 (2018).
- [26] Yu. A. Bychkov and É. I. Rashba, Properties of a 2D electron gas with lifted spectral degeneracy, *JETP Lett.* **39**, 78 (1984).
- [27] M. C. Gutzwiller, *Chaos in Classical and Quantum Mechanics* (Springer-Verlag, New York, NY, 1990).
- [28] O. Bohigas, M. J. Giannoni, and C. Schmit, Characterization of chaotic quantum spectra and universality of level fluctuation laws, *Phys. Rev. Lett.* **52**, 1 (1984).
- [29] T. A. Brody, A statistical measure for the repulsion of energy levels, *Lett. Nuovo Cimento* **7**, 482 (1973).
- [30] P. W. Anderson, Absence of diffusion in certain random lattices, *Phys. Rev.* **109**, 1492 (1958).
- [31] V. Uchaikin and R. Sibatov, *Fractional Kinetics in Solids: Anomalous Charge Transport in Semiconductors, Dielectrics, and Nanosystems* (World Scientific, Singapore, 2013).
- [32] A. A. Abrikosov, L. P. Gorkov, and I. E. Dzyaloshinskii, *Methods of Quantum Field Theory in Statistical Physics* (Dover, New York, NY, 1975).
- [33] B. L. Altshuler and A. G. Aronov, *Electron-Electron Interaction in Disordered Conductors* (Elsevier, Amsterdam, 1985).
- [34] *Handbook of Mathematical Functions*, edited by M. Abramowitz and I. Stegun (Dover, New York, NY, 1972).
- [35] P. D. Ditlevsen, Anomalous jumping in a double-well potential, *Phys. Rev. E* **60**, 172 (1999).
- [36] R. P. Feynman and A. R. Hibbs, *Quantum Mechanics and Path Integrals* (McGraw-Hill, New York, NY, 2005).
- [37] Z. Yue, V. V. Mkhitarian, and M. E. Raikh, Spectral narrowing and spin echo for localized carriers with heavy-tailed Lévy distribution of hopping times, *Phys. Rev. B* **93**, 195319 (2016).
- [38] V. A. Stephanovich and W. Olchawa, Lévy distributions and disorder in excitonic spectra, *Phys. Chem. Chem. Phys.* **22**, 24462 (2020).
- [39] C. Grimaldi, Energy levels of a two-dimensional hydrogen atom with spin-orbit Rashba interaction, *Phys. Rev. B* **77**, 113308 (2008).
- [40] E. V. Kirichenko and V. A. Stephanovich, The influence of disorder on the exciton spectra in two-dimensional structures, *Phys. Chem. Chem. Phys.* **21**, 21847 (2019).
- [41] E. V. Kirichenko and V. A. Stephanovich, The influence of Coulomb interaction screening on the excitons in disordered two-dimensional insulators, *Sci. Rep.* **11**, 11956 (2021).
- [42] V. A. Stephanovich, W. Olchawa, and E. V. Kirichenko, Screened Coulomb interaction in insulators with strong disorder, *Phys. Rev. E* **107**, 054141 (2023).
- [43] L. D. Landau and E. M. Lifshits, *Quantum Mechanics, Nonrelativistic Theory* (Pergamon Press, Oxford, UK, 1995).
- [44] X. L. Yang, S. H. Guo, F. T. Chan, K. W. Wong, and W. Y. Ching, Analytic solution of a two-dimensional hydrogen atom. I. Nonrelativistic theory, *Phys. Rev. A* **43**, 1186 (1991).
- [45] V. A. Stephanovich, On the discrete spectrum of fractional quantum hydrogen atom in two dimensions, *Phys. Scr.* **94**, 125108 (2019).
- [46] V. A. Stephanovich, E. V. Kirichenko, V. K. Dugaev, J. H. Saucó and B. López Brito, Fractional quantum oscillator and disorder in the vibrational spectra, *Sci. Rep.* **12**, 12540 (2022).
- [47] E. Ott, *Chaos in Dynamical Systems* (Cambridge University Press, Cambridge, UK, 1993).
- [48] A. Yamakage, K. Nomura, K.-I. Imura and Y. Kuramoto, Criticality of the metal-topological insulator transition driven by disorder, *Phys. Rev. B* **87**, 205141 (2013).
- [49] F. J. Dyson, Statistical theory of the energy levels of complex systems, *J. Math. Phys.* **3**, 140 (1962).
- [50] T. Ando, A. B. Fowler and F. Stern, Electronic properties of two-dimensional systems, *Rev. Mod. Phys.* **54**, 437 (1982).
- [51] N. S. Rytova, Screened potential of a point charge in a thin film, *Proc. MSU Phys. Astron.* **3**, 30 (1967); see also [arXiv:1806.00976](https://arxiv.org/abs/1806.00976) for its recent translation into English; L. V. Keldysh, Coulomb interaction in thin semiconductor and semimetal films, *JETP Lett.* **29**, 658 (1979).
- [52] P. Cudazzo, I. V. Tokatly and A. Rubio, Dielectric screening in two-dimensional insulators: Implications for excitonic and impurity states in graphane, *Phys. Rev. B* **84**, 085406 (2011).
- [53] E. V. Kirichenko, V. A. Stephanovich and E. Y. Sherman, Chaotic cyclotron and Hall trajectories due to spin-orbit coupling, *Ann. Phys.* **532**, 2000012 (2020).
- [54] M. A. Semina, M. M. Glazov, and E. Sherman, Interlayer exciton-polaron in atomically thin semiconductors, *Ann. Phys.* **532**, 2000339 (2020).
- [55] Z. A. Iakovlev, M. A. Semina, M. M. Glazov and E. Y. Sherman, Flexural deformations and collapse of bilayer two-dimensional crystals by interlayer excitons, *Phys. Rev. B* **105**, 205305 (2022).
- [56] A. M. Kosevich, *The Crystal Lattice: Phonons, Solitons, Dislocations* (Wiley, Berlin, 1999).